JOURNAL OF MATERIALS SCIENCE 13 (1978) 691–701

The role of dislocations in the precipitation of $M_{23}C_6$ in Co-Cr-C alloys

P. A. BEAVEN*
Department of Metallurgy and Materials Science, University of Oxford, UK

P. R. SWANN, D. R. F. WEST
Department of Metallurgy and Materials Science, Imperial College, London, UK

An investigation is reported of the mechanisms of $M_{23}C_6$ precipitation from supersaturated f c c solid solution in two Co–Cr–C alloys of compositions (wt %): Co–25.3 Cr–0.26 C and Co–32.9 Cr–0.18 C. Electron microscope investigations were made with particular reference to the role of dislocations in the nucleation and growth of carbide particles formed on ageing in the range 650 to 800° C. Carbide precipitation occurred initially as a fine homogeneously distributed dispersion of matrix-nucleated particles. Extrinsic stacking faults were nucleated at some of the matrix particles. Stacking faults grew and repeated carbide precipitation occurred on the bounding Frank partials. The fault density increased with ageing time, and various stacking fault interactions were observed. Carbide precipitation occurred also on undissociated dislocations and on Shockley partials.

1. Introduction

The structural and kinetic features of carbide precipitation from f c c matrices are of considerable interest in relation to the development of desirable mechanical properties in various alloys used at elevated temperatures. In this context, austenitic steels have been studied in considerable detail, and various modes of precipitation from supersaturated solid solutions have been identified and analysed [1–3]. Carbide precipitation phenomena in both f c c and h c p cobalt-based superalloys have been studied to a limited extent [4–10], and offer an interesting comparison with the austenitic steels. Previously reported work has included a study of the structure and strength of two precipitation-hardened Co–Cr–C alloys [7] (Co–25.3 wt % Cr–0.26 wt % C; Co–32.9 wt % Cr–0.18 wt % C). On ageing in the range 650 to 800° C both matrix and dislocation-nucleated precipitation of $M_{23}C_6$ were observed and in the alloy of higher chromium content a cellular mode of precipitation also occurred.

The present paper is concerned mainly with detailed observations of the role of dislocations in the nucleation and growth of carbide particles during the ageing of these same alloys.

2. Experimental procedure

The alloys of composition (wt %) Co–25.3 Cr–0.26 C and Co–32.9 Cr–0.18 C respectively, were prepared by CNRM, Belgium, and were received in wrought form. Strip samples were sealed in silica capsules under $\frac{1}{3}$ of an atmosphere of high purity argon; they were generally solution treated for 1 h at 1300° C followed by water quenching, the capsules being broken under the water surface. Some experiments were made involving air cooling from 1300° C, or water quenching from 1200° C. Ageing treatments were carried out in the range 650 to 1000° C, with the specimens sealed in silica capsules under argon.

Specimens for electron microscopy were prepared by electropolishing discs (~0.01 mm thick)

*Formerly in the Department of Metallurgy and Materials Science, Imperial College, London, UK.

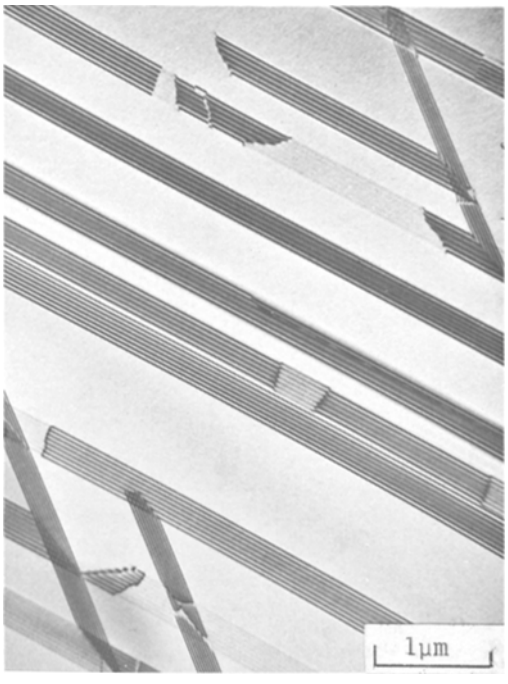

Figure 1 Co–25.3 Cr–0.26 C alloy, solution treated for 1 h at 1300° C, and water quenched. Bright-field micrograph showing overlapping stacking faults (intrinsic).

using a jetting technique with a 20% perchloric acid/80% acetic acid solution at ~15° C.

3. Experimental results

3.1. Solution-treated specimens

The structures of specimens as-quenched from 1300° C were f c c, with a grain size of the order of 0.1 mm and a small amount of carbide remaining undissolved. There was an inhomogeneous dislocation sub-structure, in some regions dislocations being widely dissociated, while in others they were undissociated. This marked variation rendered impracticable the measurement of stacking fault energy; clearly the stacking fault energy was very small and it appeared that the equilibrium separation of the partials was difficult to achieve. Clusters of overlapping faults were a common feature (Fig. 1). Using established methods [11, 12] and taking care to ensure that only single faults were analysed, the faults were shown to be intrinsic. The density of faults was related primarily to the distribution and amount of undissolved carbide particles, and a high density of faults existed around these particles.

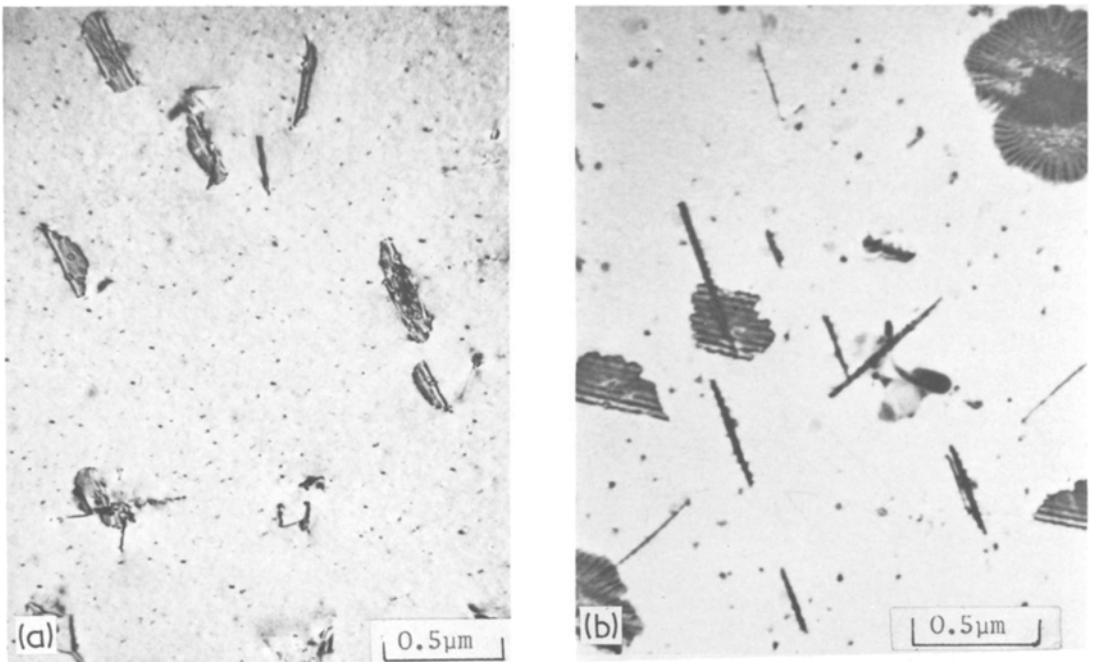

Figure 2 Co–25.3 Cr–0.26 C alloy. (b) Co–32.9 Cr–0.18 C alloy. Both alloys were solution treated for 1 h at 1300° C, and water quenched. Aged 5 h at 700° C. Bright-field micrographs showing $C_{23}C_6$ precipitation in matrix and on partial dislocations, in association with stacking faults; in (b) ribbon shaped particles are present in the stacking faults.

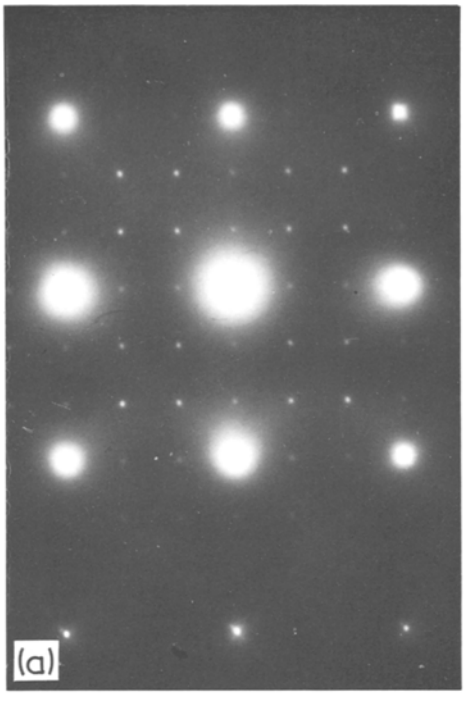

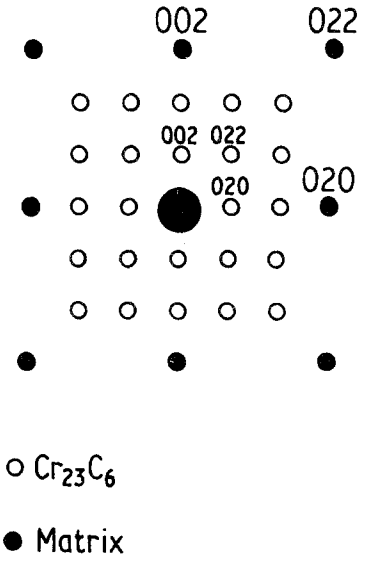

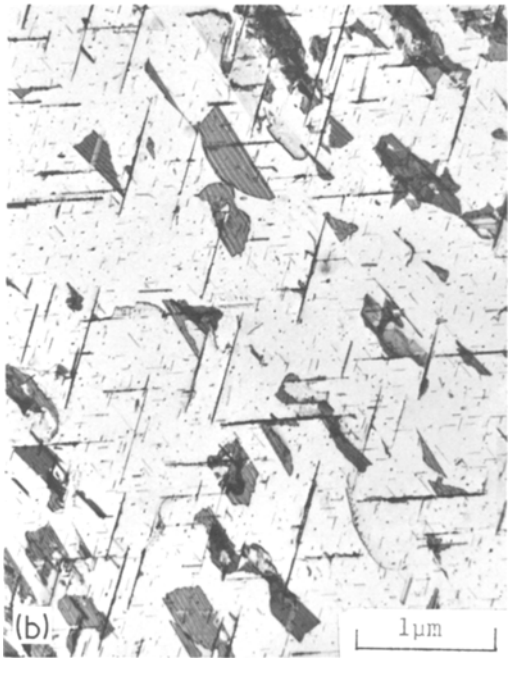

Figure 3 Co–25.3 Cr–0.26 C alloy solution treated for 1 h at 1300° C and aged 20 h at 700° C. (a) SADP showing $Cr_{23}C_6$ in cube–cube orientation relationship with the matrix. (b) Bright-field micrograph showing rod-like morphology of matrix precipitates, with growth preferred in the ⟨1 1 0⟩ direction; also numerous stacking faults are present; foil orientation ~(1 1 0).

3.2. Precipitation in the matrix

The structural features can be well illustrated by reference to specimens aged in the range 650 to 800° C. Carbide precipitation occurred initially in the matrix as a fine, homogeneously distributed dispersion. Faulted dislocation loops developed, decorated with particles formed by repeated nucleation on the partial dislocations bounding the faults.

Figs. 2a and b represent the structures of the higher and lower carbon alloys in the early stages of ageing at 700° C and show the homogeneously distributed dispersion of fine precipitate particles in the matrix and also faulted loops decorated with particles. The density of matrix particles and of faulted loops was greater in the higher carbon alloy; however, because of this greater degree of matrix precipitation the proportion of carbide precipitated on dislocations was less.

The matrix particles were revealed by strain field contrast. In the earliest stages in the higher carbon alloy, the line of no-contrast was perpendicular to the **g**-vector of the operating reflection, indicating a spherically symmetrical strain field. In the lower carbon alloy, even for the shortest time examined, i.e. 2 h, the line of no-contrast was not perpendicular to the operating reflection suggesting that the particle shape was no longer

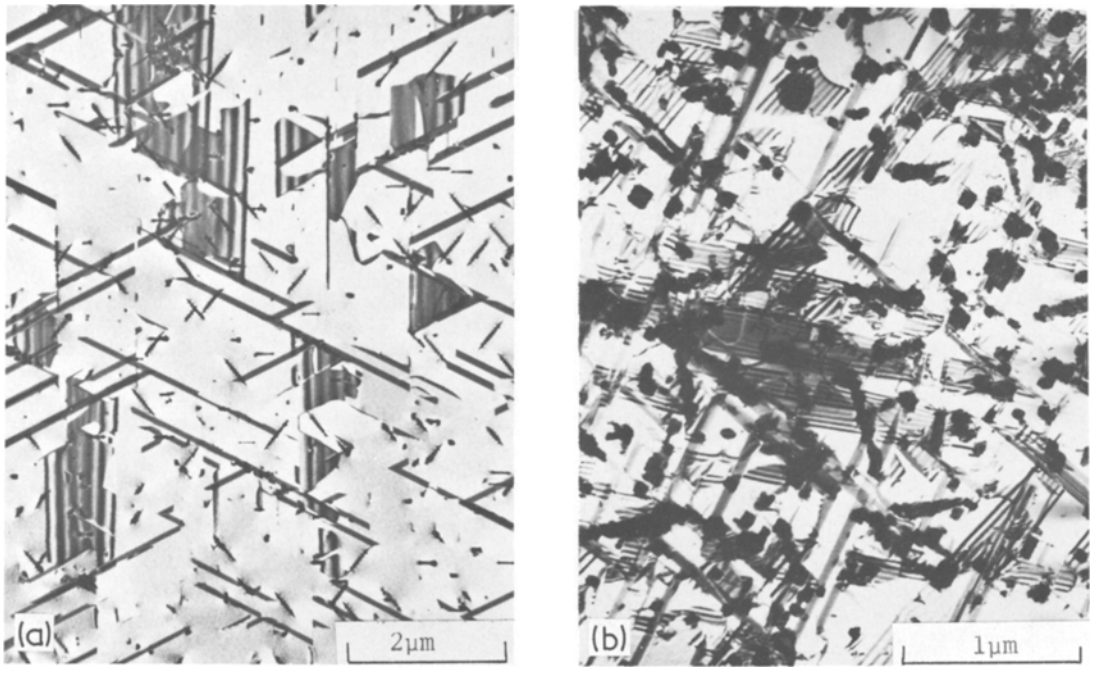

Figure 4 Co–32.9 Cr–0.18 C alloy, solution treated for 1 h at 1300° C and water quenched. (a) Aged 1 h at 800° C. Bright-field micrograph showing rod-like precipitates in the matrix surrounded by arrays of dislocation loops; numerous stacking faults are present. (b) Aged 20 h at 800° C. Bright-field micrograph showing angular particles in the matrix.

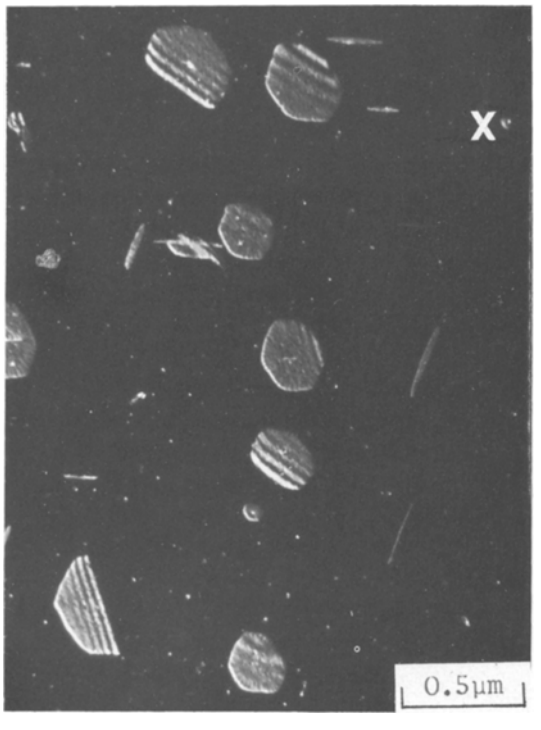

Figure 5 Co–32.9 Cr–0.18 C alloy solution treated for 1 h at 1300° C, and water quenched. Aged 2 h at 700° C. Dark-field micrograph showing stacking faults nucleated at matrix precipitate particles; X shows a faulted loop at an early stage of formation; $\mathbf{g} = 0\,0\,2$.

spherical or that a dislocation loop had formed at the precipitate/matrix interface.

After 20 h ageing at 700° C (Fig. 3a), precipitate reflections were clearly visible on diffraction patterns; both the homogeneously distributed precipitate and that heterogeneously nucleated were identified as $Cr_{23}C_6$ with $a = 10.64$ Å showing a cube–cube orientation relationship with the matrix. At this stage of ageing in both alloys (Fig. 3b) the matrix precipitates had adopted a rod-like morphology, with growth preferred in the $\langle 1\,1\,0 \rangle$ directions.

The elongation of matrix nucleated particles in $\langle 1\,\bar{1}\,0 \rangle$ directions (dimensions ~ 7500 Å × 2000 Å × 2000 Å) is also illustrated in a specimen of the Co–32.9 Cr–0.18 C alloy aged for 1 h at 800° C (Fig. 4a). Coherency had been lost, and the laths were surrounded by arrays of dislocation loops, with a spacing of ~400 Å. Lattice parameter data (matrix $a \sim 3.565$ Å; $Cr_{23}C_6 = 10.623$ Å) give a mismatch of 0.67% which could be accommodated by a parallel array of $a/2\langle 1\,1\,0 \rangle$ dislocations with a spacing of ~ 380 Å. The ends of the long particles appear to be curved, a feature also noted by Singhal and Martin [13] during a study of matrix precipitation of $M_{23}C_6$ in austenite. With continued ageing (e.g. 24 h at 800° C) thickening of

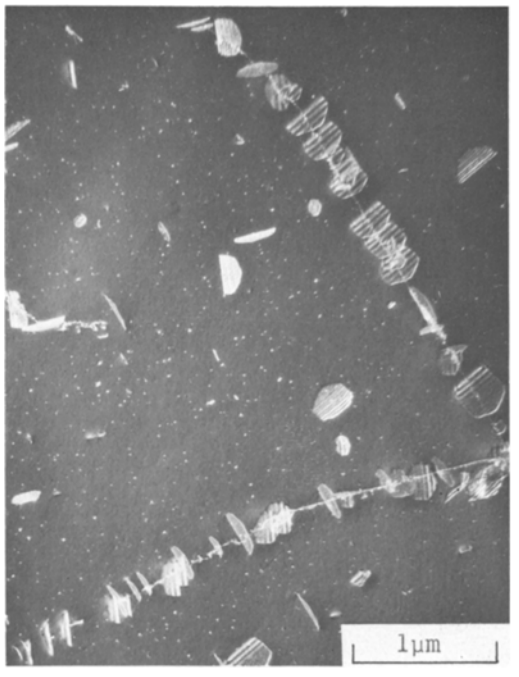

Figure 6 Co–32.9 Cr–0.18 C alloy, solution treated for 1 h at 1300° C and water quenched. Aged 2 h at 700° C. Dark-field micrograph showing development of extrinsic stacking faults from carbide particles on originally undissociated dislocations.

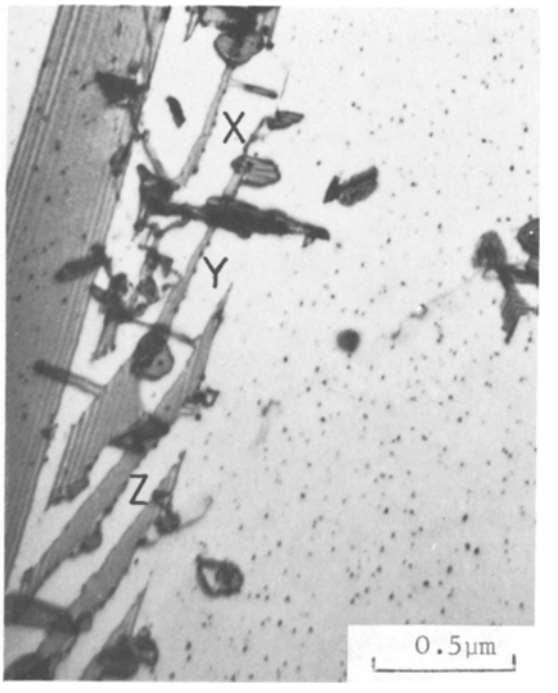

Figure 7 Co–25.3 Cr–0.26 C solution treated for 1 h at 1300° C and water quenched. Aged 24 h at 650° C. Bright-field micrograph showing carbide nucleation at Shockley partials X, Y and Z, g = 0 2 2.

the matrix particles occurred, producing angular shapes (Fig. 4b) with interface planes of the {1 1 1} type.

Some observations were made on specimens of the Co–32.9 Cr–0.18 C alloy to explore the effect of air cooling from the solution treatment temperature and also the effect of reducing the solution treatment temperature from 1300 to 1200° C, but still employing water quenching. On ageing for 5 h at 700° C after air cooling from 1300° C, there was no detectable change in the rate of nucleation of the matrix precipitate or in the number of stacking faults formed. In a specimen water quenched after 1 h at 1200° C and then aged for 2 h at 700° C there was an almost complete absence of matrix precipitation, and a reduced rate of growth of the few stacking faults present.

3.3. Stacking fault nucleation

Detailed observations were made of the formation and growth of the stacking faults, during ageing, and of their associated precipitates. Using established methods [11, 12] the faults were shown to be extrinsic in nature and their "outer" boundaries were Frank partial dislocations. A small loop was sometimes observed at the centre of the faults which was found to be a Shockley partial dislocation of Burgers vector $a/6\,[1\,\bar{2}\,1]$; however, this loop was often too small to be studied. Growth of the faults occurred by the mechanism proposed by Silcock and Tunstall [14].

It was concluded that extrinsic faults were nucleated at matrix precipitate particles (Fig. 5), and there was frequently a larger-than-average carbide particle at the centre of the faults. In Fig. 5 the diameters of the stacking fault loops range up to ~4000 Å and the region marked X shows a faulted loop at an early stage of formation.

In a few instances dislocations were observed that appeared to be undissociated, and on which arrays of extrinsic faults formed. Examination under different conditions of tilting established that very little climb of the original dislocation occurred, and that fault formation was usually associated with Frank partials generated from $Cr_{23}C_6$ precipitates (Fig. 6). The relative rates of precipitate nucleation appeared to be strongly

influenced by the character of the dislocation, and this in turn affected the number of extrinsic faults formed at a particular dislocation.

Fig. 7 shows the occurrence of carbide nucleation on Shockley partials; a complex array of intrinsic and extrinsic faults is seen. Contrast analysis of the partial dislocations at X, Y and Z, etc. showed them to be Shockley partials. Precipitate nucleation had occurred on these, and furthermore extrinsic fault formation had occurred round these particles in some cases. The particles appear to have nucleated on only one partial of each dissociated dislocation, and it therefore remains a possibility that dissociation occurred after carbide nucleation on an apparently undissociated dislocation. If this were true, dissociation could only have occurred by glide since the fault was intrinsic and bounded by Shockley partials. In a number of cases dislocation dipoles appeared to have formed at the Shockley partials, but insufficient evidence was obtained to explain this behaviour. It is thus concluded that extrinsic fault nucleation occurred predominantly in association (1) with precipitate particles that may have nucleated in the matrix, (2) on Shockley partial dislocations or (3) on undissociated dislocations.

Figure 8 Co–32.9 Cr–0.18 C alloy solution treated for 1 h at 1300° C and water quenched. Aged 5 h at 700° C. Bright-field micrograph showing stacking faults with clusters of ribbon shaped particles, g = 131.

3.4. Stacking fault growth and repeated nucleation

In both alloys the apparent fault density increased with increase in ageing time. In the higher carbon alloy the faults grew with relatively little repeated nucleation on the partials, but in the lower carbon alloy repeated nucleation commonly occurred [14]. In this latter alloy the larger faults contained coarser particles than those in the faults at an earlier stage of growth; this indicates that growth continued after the expanding Frank partial had moved on from each row of particles. The average particle diameter in the earliest stages was ~80 Å, and the average interparticle spacing was ~400 Å, being similar in directions normal and parallel to the Frank partial.

As the ageing time in the Co–32.9 Cr–0.18 C alloy increased, the partial dislocations became serrated. This is illustrated in Fig. 2b, in which the stacking faults contain clusters of discrete particles at their centres, with lines of contrast emanating radially. In Fig. 8, the normal fault fringes are not in strong contrast, and examination with $\mathbf{g} = 0\,0\,2$ showed that the Frank partial was continuous around the fault. The lines of dark contrast radiating from the centre of the fault and lying perpendicular to the Frank partial are thin "ribbons" of $Cr_{23}C_6$. This ribbon formation and the serrations of the Frank partials occurred to a greater extent at 650° C than at 700° C, but did not occur at 800° C, at which temperature fault growth proceeded without further precipitation. The Co–25.3 Cr–0.26 C alloy did not show ribbon formation.

In both alloys there were a few instances of precipitation associated with climb at apparently undissociated dislocations, e.g. Fig. 3b; arrays of fine equiaxed particles formed, lying on {1 1 0} matrix planes, with the Burgers vector of the dislocations lying in a direction normal to the plane of movement indicating that climb had occurred.

3.5. Stacking fault interactions

Complex interactions of the faults occurred with increase in ageing time. For example, Fig. 9a shows a high density of faults in the Co–25.3 Cr–0.26 C alloy aged 100 h at 700° C; extensive streaking was produced along ⟨1 1 1⟩ in diffraction patterns.

Fig. 9b shows a similar structure in the Co–32.9 Cr–0.18 C alloy aged for 1 h at 800° C; a

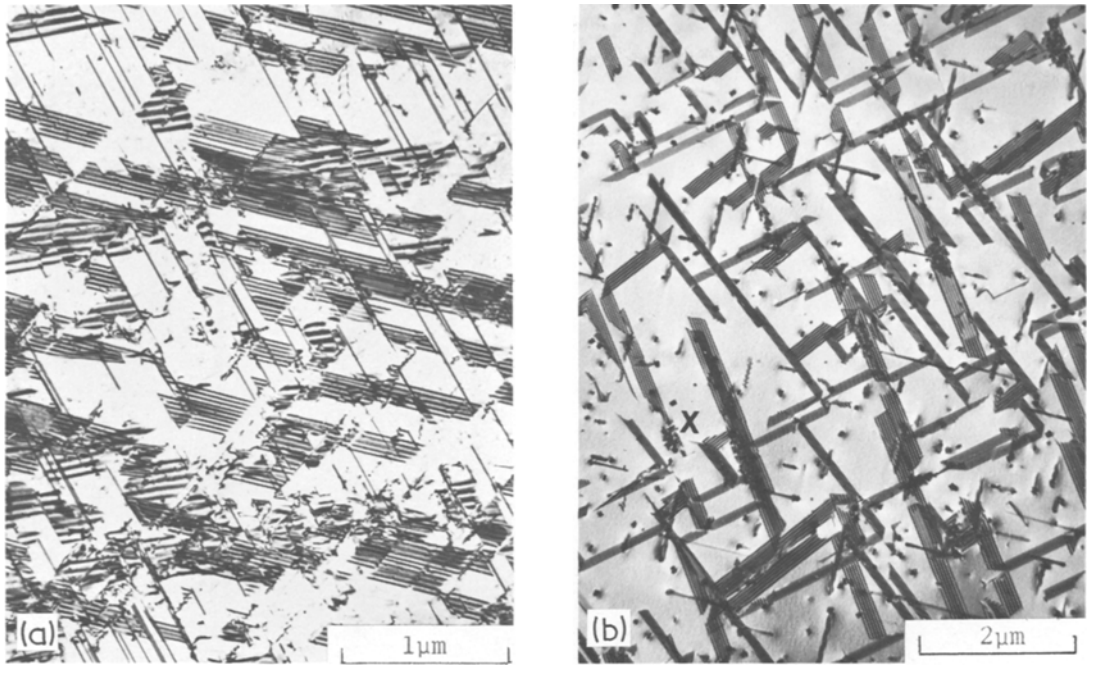

Figure 9 (a) Co–25.3 Cr–0.26 C alloy solution treated for ~1 h at 1300° C and water quenched. Aged 100 h at 700° C. Bright-field micrograph showing high density of stacking faults. (b) Co–32.9 Cr–0.18 C alloy solution treated for 1 h at 1300° C and water quenched. Aged 1 h at 800° C. Bright-field micrograph showing fault–fault and fault–precipitate interactions, e.g. at X, fault cancellation has occurred around clusters of carbide particles nucleated by Frank partials.

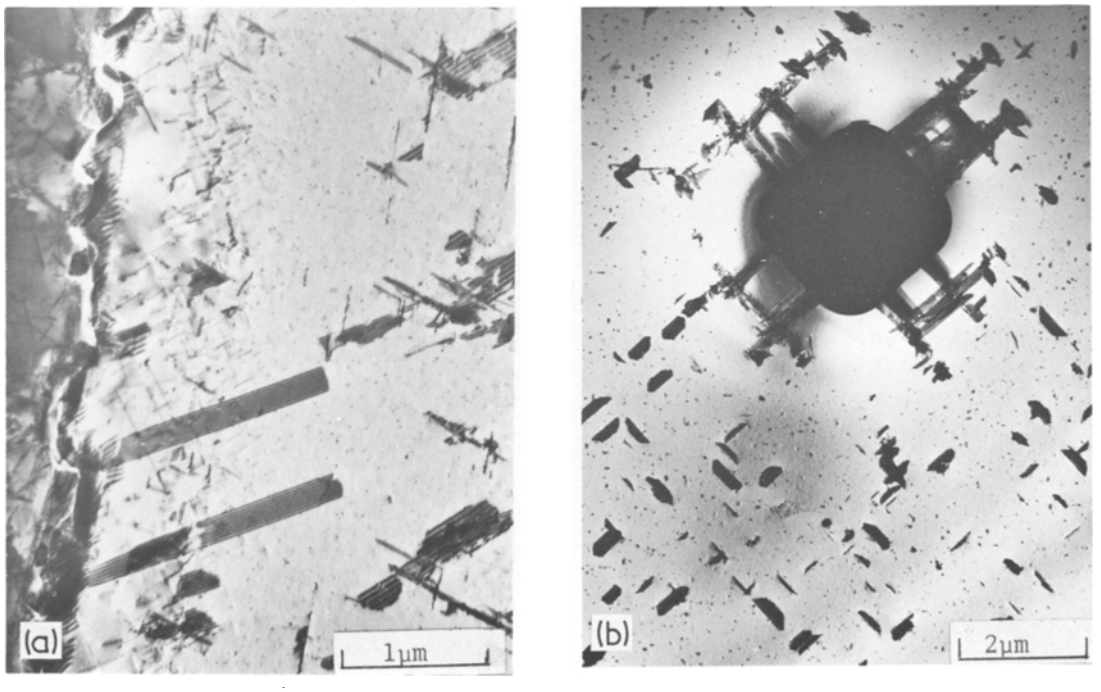

Figure 10 (a) Co–25.3 Cr–0.26 C alloy solution treated for 1 h at 1390° C and water quenched. Aged 20 h at 700° C. (b) Co–32.9 Cr–0.18 C alloy solution treated for 1 h at 1300° C and water quenched. Aged 2 h at 700° C. Bright-field micrographs showing distribution of stacking faults and precipitates in the region of a grain boundary and an undissolved carbide particle respectively.

number of features are apparent in the complex stacking fault interactions:

(1) The partial dislocations bounding the faults often lie along ⟨1 1 0⟩ matrix directions and are invisible with $\mathbf{g} = 0\,0\,2$; this indicates that in such cases the dislocations are no longer Frank partials, dissociation of the Frank partial dislocations having occurred. The dissociation produces a low energy stair-rod dislocation and a Shockley partial which is glissile on an intersecting {1 1 1} plane. Further fault growth occurs by glide of the Shockley partial, thus giving rise to the bending of faults commonly observed. This dissociation of the Frank partials appears to occur where faults meet precipitate particles or other faults.

(2) High resolution dark-field studies show that both extrinsic and intrinsic faults are present at this stage of ageing.

(3) Fault cancellation can occur around clusters of carbides nucleated by the Frank partials, e.g. at X. This occurs relatively infrequently in contrast to the behaviour in austenitic steels, where stacking fault contrast disappears as the associated precipitate particles undergo coarsening.

3.5. The role of grain boundaries and undissolved carbide particles.

Fig. 10a illustrates the precipitate and stacking fault distribution close to a grain boundary in a specimen of the Co–25.3 Cr–0.26 C alloy aged for 20 h at 700° C. Coarse particles of $Cr_{23}C_6$ were present on the grain boundary, with an adjoining zone (of width ~0.4 μm) free of matrix precipitates. Adjacent to this was a region of enhanced precipitation in which the carbide particles were predominantly rod-like, and there followed a region which was largely devoid of extrinsic stacking faults. The width of this region was found to be temperature-dependent and varied from 1 μm at 700° C to 2 μm at 800° C. Air cooling instead of water quenching from the solution treatment temperature led to an increase in the width of this region on ageing. There was also a tendency for the precipitate-free zone to decrease with ageing time as growth of the rods continued towards the grain boundary. The higher chromium alloy showed similar grain boundary precipitation effects.

Fig. 10b shows the influence of undissolved carbide particles on the distribution of precipitates and stacking faults. A zone depleted in matrix precipitates exists around the large carbide particle. Intrinsic stacking faults were generated by this particle during quenching from the solution treatment temperature; on ageing, carbide precipitation occurred on the Shockley partials, and these carbide precipitates gave rise to the generation of extrinsic stacking faults with associated precipitation on the Frank partials (see Fig. 7).

4. Discussion

4.1. Matrix precipitation

Previous work, e.g. on aluminium alloys [15] and stainless steels [16] has shown that matrix precipitation is dependent on the concentration and distribution of quenched-in vacancies. The fact that the particle density formed on ageing the Co–32.9 Cr–0.18 C alloy was hardly changed by air cooling from 1300° C instead of water quenching may be associated with the formation of metal–carbon–vacancy complexes at relatively high temperatures, in a manner comparable with observations on certain austenitic stainless steels (e.g. [17]). In the absence of such complexes air cooling would be expected to reduce the concentration of quenched-in vacancies and hence the tendency to matrix precipitation; however, if there is a tendency to complex formation this will be aided by a reduction in the cooling rate and the complexes will assist matrix precipitation. The reduction in particle density and the reduced rate of precipitation observed after solution treatment at 1200° C and ageing may then be attributed to a reduction in vacancy concentration, rather than to the slight decrease in solute supersaturation due to the greater amount of undissolved particles.

Direct ageing experiments to determine the critical temperature for matrix precipitation, T_c, have not been carried out in the present work. The occurrence of matrix nucleation at 1000° C is likely to result from nucleation during heating, with growth occurring at 1000° C.

4.2. Coherency loss and the nucleation of extrinsic loops

The results show that the formation of extrinsic stacking faults is linked with the mechanism of coherency loss of the matrix precipitates. This also appears to hold when the initial precipitates are formed on dislocations.

The loss of coherency in growing precipitate particles has been studied by a number of workers

(e.g. [18–25]), and various models have been proposed for the "critical misfit" required to cause dislocation generation at a misfitting particle. In the present alloys, the value of the mismatch (misfit), ϵ, calculated from the difference in metal atom volume between $Cr_{23}C_6$ and the matrix is ~0.03. This value is in reasonable agreement with the conditions discussed by Ashby and Johnson [23] for loss of coherency by dislocation generation.

The formation of extrinsic loops around matrix nucleated particles has been observed to occur infrequently during $M_{23}C_6$ precipitation in austenitic steels [26] and these loops were not observed to be formed by the climb of decorated, perfect dislocations; this supports the present observations, indicating that the volume change associated with $Cr_{23}C_6$ precipitation is not sufficient to force an initially undissociated dislocation into a suitable orientation for the dissociation to a Frank partial dislocation to take place. From the observation of extrinsic loops at isolated matrix particles of V_4C_3 in austenite, as well as in association with decorated dislocations, Silcock [27] has suggested that a Frank loop forms directly at the particle/matrix interface, rather than a perfect loop. The present results suggest that either of these possibilities can occur, as in some instances a Shockley loop was observed around the central particle, whereas in other instances only the surrounding Frank partial was noted.

Only a small fraction of the matrix precipitates produced extrinsic loops, and the number of faults appears to be related to the density of matrix precipitates. This suggests that the same factors control both the matrix precipitate density and the stacking fault density, i.e. the quenched-in vacancy concentration and the solute supersaturation. Thus the fault density depends on solution treatment temperature, and ageing temperature.

The role of pre-existing imperfections, i.e. dislocations and Shockley partial dislocations, in aiding stacking fault nucleation is primarily "kinetic". Precipitates formed on dislocations are supplied with solute by pipe diffusion, thus allowing the critical particle size for loop formation to be reached at an early stage in ageing. In cases where whole dislocation climb was noted, this invariably led to arrays of particles on {1 1 0} planes, and not to stacking fault formation.

4.3. Stacking fault growth

The stacking fault precipitation process occurred by the mechanism proposed by Silcock and Tunstall [14], who calculated that the Frank partials are able to move away from the associated precipitate particles when the linear strain caused by the particle is equal to the Burgers vector. For $Cr_{23}C_6$ the volume expansion is ~12%, and the linear strain equivalent to the Burgers vector of the Frank partial is produced by a particle diameter of ~50 Å. The smallest particles of $Cr_{23}C_6$ observed on the faults were ~80 Å but it should be borne in mind that some growth has occurred after the Frank partial has climbed away.

Using the model of Silcock and Tunstall [14] it can be calculated that for $Cr_{23}C_6$ in austenite, climb will occur provided that the gap between particles is less than 1.9 times their length. In general, for the present alloys, the precipitate distribution was very irregular, and this criterion was not satisfied. It appears that climb can occur more easily, due to the presence of vacancy sinks, such as matrix particles, that serve to maximize the climb force on the partials. The fault energy is considerably lower in cobalt alloys than in austenitic steels and this may also facilitate climb.

When the faults reach a size of ~3000 to 4000 Å, repeated nucleation ceases. In the lower carbon alloy at 650 and 700° C this produced ribbons of precipitate normal to the partial dislocations. Thus the nucleation rate at the partials decreases as the matrix solute concentration decreases and the partials become serrated since they cannot climb uniformly away from the last row of precipitates. Solute is transported by pipe diffusion to the existing particles which grow as thin lamellae, the supersaturation being insufficient for the nucleation of discrete particles. A similar effect has been observed for $Cr_{23}C_6$ precipitation in austenitic steels [26]; another effect involving the formation of precipitate ribbons along Frank partials has been reported for NbN precipitation in austenitic steels [28].

Continued climb of the Frank partial is thought to arise from the decreasing stacking fault energy of the matrix. This is particularly apparent during ageing of the lower carbon alloy at 800° C when fault growth continues in the absence of ribbon formation. In some cases this apparently occurred by glide, due to the dissociation of the Frank partial by the reaction:

$$a/3\ [1\,1\,\bar{1}] \rightarrow a/6\ [1\,1\,0] + a/6\ [1\,1\,\bar{2}]$$

This produces a sessile stair rod dislocation and a Shockley partial which is glissile on an intersecting $\{1\,1\,1\}$ plane. At this stage the discontinuous precipitation reaction: austenite $\rightarrow$ ϵ phase + $M_{23}C_6$ has commenced and the matrix is metastable with respect to the allotropic transformation; this may produce the driving force for fault growth, since stacking faults can be considered as a thin lamellae of h c p ϵ phase. At lower temperatures the aggregates of ribbons in association with the faults resemble a cellular reaction in two dimensions. A similar process has been observed in Cu–Ag alloys [29], and certain austenitic steels. It seems that there is an analogy between the formation of a lamellar precipitate in association with both a moving dislocation and a moving grain boundary, since both provide enhanced diffusivity and accommodation of strain.

The results show that repeated nucleation of $Cr_{23}C_6$ can occur only to a limited extent. For a high density of faults to form, a high density of matrix particles is required, but in these circumstances repeated nucleation is not favoured, due to the rapid decrease in solute supersaturation.

4.4. Precipitation in grain boundary regions

The presence of zones free of matrix precipitates, adjacent to grain boundaries, (and to undissolved carbide particles) is attributed to vacancy depletion rather than solute depletion. The carbides on the edge of the PFZs were slightly coarser than those in the matrix, indicating that these particles draw solute from within the PFZ [2, 13]. With increasing ageing time the presence of a zone of enhanced precipitation on the edge of the PFZ may result from grain boundaries acting as vacancy sources, thus increasing the diffusion rate and relieving particle growth stresses in these regions.

5. Conclusions

The precipitation of $Cr_{23}C_6$ from supersaturated solid solution in the range 650 to 800° C shows the following characteristics in the alloys Co–25.3 Cr–0.26 C and Co–32.9 Cr–0.18 C:

(1) Precipitation commences in the matrix as a fine, homogeneous dispersion of coherent spherical shaped particles. The number density of these particles is greater in the higher carbon alloy.

(2) As ageing proceeds, matrix particles adopt a rod-like morphology with growth preferred in the $\langle 1\,1\,0 \rangle$ directions; coherency loss occurs and arrays of dislocation loops surround the particles. Eventually, the matrix precipitates thicken to form angular shapes.

(3) For a small proportion of the matrix particles, loss of coherency (occurring at <100 Å diameter) leads to the formation of faulted loops around the particles, these faults being extrinsic; the density of faults is greater in the higher carbon alloy.

(4) The number of faults appears to be related to the density of matrix precipitates, suggesting the same controlling factors for precipitate and fault formation, i.e. quenched-in vacancy concentration and solute supersaturation.

(5) The outer boundaries of the faults are Frank partials, and fault growth commonly occurs by the mechanism proposed by Silcock and Tunstall, involving repeated nucleation of precipitate particles. In the higher carbon alloy the faults grow with relatively little nucleation on the partials, and in the lower carbon alloy, at 650 and 700° C the partials become serrated and the particles become ribbon shaped.

(6) To obtain a high density of faults a high matrix density is needed, but the resultant decrease in solute supersaturation does not favour the occurrence of repeated nucleation on partials.

(7) Complex interactions between faults and between faults and precipitates occur.

(8) Precipitate formation associated with climb occasionally occurs at undissociated dislocations.

(9) Vacancy effects, e.g. PFZs, occur in the grain boundary regions.

(10) In the higher chromium alloy a discontinuous precipitation reaction occurs at long ageing times.

Acknowledgements

Acknowledgements are made to Professor J. G. Ball for the provision of research facilities; to CNRM, by arrangement of Mr J. Williams, for the supply of the alloys, and to the Science Research Council for the award of a research studentship to one of the authors (PAB). The work formed part of a thesis submitted by one of the authors (PAB) for the PhD degree of London University.

References

1. J. S. T. VAN ASWEGAN, R. W. K. HONEYCOMBE and D. H. WARRINGTON, *Acta Met.* **12** (1964) 1.
2. F. H. FROES, R. W. K. HONEYCOMBE and D. H. WARRINGTON, *ibid* **15** (1967) 157.

3. J. M. SILCOCK and A. W. DENHAM, "The Mechanism of Phase Transformations in Crystalline Solids" (Institute of Metals, London, 1968) p. 59.
4. P. S. KOTVAL, *Trans. AIME* **242** (1968) 1651.
5. P. S. KOTVAL, *Metallography* **1** (1969) 251.
6. V. RAMASWAMY, P. R. SWANN and D. R. F. WEST, Seventh International Conference of Electron Microscopy, Grenoble, 1970, p. 543.
7. *Idem,* Proceedings of the Fifth International Symposium, University of California, Berkeley, 1971, p. 637.
8. *Idem.* Third International Conference on the Strength of Metals and Alloys, Cambridge, 1973, p. 340.
9. J. B. VANDER SANDE, J. R. COKE and J. WULFF, *Met. Trans. AIME* **7A** (1976) 389.
10. J. H. DAVIDSON, Third International Symposium on Superalloys, *Met. Soc. AIME* (1976) 275.
11. H. HASHIMOTO, M. M. MANNAMI and T. NAIKI, *Proc. Roy. Soc.* **A269** (1962) 80.
12. R. GEVERS, A. ART and S. AMELINCKX, *Phys. Stat. Sol.* **3** (1963) 1563.
13. L. K. SINGHAL and J. W. MARTIN, *Acta Met.* **16** (1968) 1159.
14. J. M. SILCOCK and W. J. TUNSTALL, *Phil. Mag.* **11** (1964) 361.
15. J. D. EMBURY and R. B. NICHOLSON, *Acta Met.* **13**, (1965) 403.
16. F. H. FROES, D. H. WARRINGTON and R. W. K. HONEYCOMBE, Proceedings of the Sixth International Congress for Electron Microscopy, Vol. I (Maruzeu Co., Tokyo, 1967) p. 431.
17. J. M. SILCOCK and A. W. DENHAM "The Mechanism of Phase Transformations in Crystalline Solids" (Institute of Metals, London, 1968) p. 59.
18. F. SEITZ, Rev. Mod. Physics, 77. (1950) 723.
19. A. EIKUM and G. THOMAS, *Acta Met.* **12** (1964) 537.
20. R. G. BAKER, D. G. BRANDON and J. NUTTING, *Phil. Mag.* 4 (1959) 1339.
21. L. M. BROWN, G. R. WOOLHOUSE and U. VALDRE, *ibid* **17** (1968) 781.
22. G. C. WEATHERLEY, *ibid* **17** (1968) 791.
23. M. F. ASHBY and L. JOHNSON, *ibid* **20** (1969) 1009.
24. L. M. BROWN and G. R. WOOLHOUSE, *ibid* **21** (1970) 329.
25. H. I. AARONSON, C. LAIRD and K. R. KINSMAN, "Phase Transformations" (ASM, Metals Park, Ohio, 1970) p. 313.
26. G. R. KEGG and J. M. SILCOCK, *Met. Sci.* **6** (1972) 47.
27. J. M. SILCOCK, *Acta Met.* **14** (1966) 687.
28. D. W. BORLAND and R. W. K. HONEYCOMBE *Met. Sci. J.* **4** (1970) 14.
29. R. RÄTY and H. M. MIEKKOJA *Phil. Mag.* **18** (1968) 1105.

Received 27 April and accepted 30 August 1977.